Chemical Science

ROYAL SOCIETY OF CHEMISTRY

EDGE ARTICLE

View Article Online
View Journal | View Issue

Cite this: *Chem. Sci.*, 2024, **15**, 16355

All publication charges for this article have been paid for by the Royal Society of Chemistry

Received 27th July 2024
Accepted 8th September 2024

DOI: 10.1039/d4sc05016a

rsc.li/chemical-science

Unravelling denaturation, temperature and cosolvent-driven chiroptical switching in peptide self-assembly with switchable piezoelectric responses†

Aparna Ramesh,‡[ab] Tarak Nath Das,‡[c] Tapas Kumar Maji *[cd] and Goutam Ghosh *[ab]

Herein, we explore the intricate pathway complexity, focusing on the dynamic interplay between kinetic and thermodynamic states, during the supramolecular self-assembly of peptides. We uncover a multiresponsive chiroptical switching phenomenon influenced by temperature, denaturation and content of cosolvent in peptide self-assembly through pathway complexity (kinetic *vs.* thermodynamic state). Particularly noteworthy is the observation of chiroptical switching during the denaturation process, marking an unprecedented phenomenon in the literature. Furthermore, the variation in cosolvent contents produces notable chiroptical switching effects, emphasizing their infrequent incidence. Such chiroptical switching yields switchable piezoresponsive peptide-based nanomaterials, demonstrating the potential for dynamic control over material properties. In essence, our work pioneers the ability to control piezoresponsive behavior by transforming nanostructures from kinetic to thermodynamic states through pathway complexity. This approach provides new insights and opportunities for tailoring material properties in self-assembled systems.

Introduction

Supramolecular assemblies with chiral helical structures, such as the double helix of DNA, the triple helix of collagen, and the α-helix of protein, are widely found in living systems and intimately associated with several biological processes.[1] Aside from improving our understanding of the role of chirality in biological contexts,[2] the helical chirality of nanoscale architectures in polymer and supramolecular self-assembly systems is crucial for expanding their application[3] in chiral recognition,[4] chiroptical switches,[5] asymmetric catalysis,[6] and optoelectronics.[7] Normal physiological processes are quickly disrupted if aberrant transitions of chiral structures take place. For instance, some oncogenes are readily activated and cancer is caused by the structural alteration of DNA from the normal right-handed helix (B-DNA) to the aberrant left-handed helix (Z-DNA).[8] Similarly, protein chain conformational disorder or chiral inversion may affect cellular processes and increase the likelihood of certain illnesses, such as Parkinson's and Alzheimer's diseases.[9] Supramolecular chirality refers to the formation of chiral helical structures in supramolecular assemblies through various non-covalent interactions.[4a,10,11] Controlling the helical sense or reversing the macroscopic chirality of nanostructures during self-assembly is a significant challenge.[4a,5b,12] However, these inversions have been achieved by modifying the chiral structures of amphiphiles,[13] adjusting the sequence of the constituents, applying various external stimuli and altering self-assembly pathways.[14–22] Supramolecular chirality inversion or switching enables dynamic modulation of material properties, offering a versatile approach to tune functionalities like optical activities, mechanical behaviors, and electronic properties. It enhances adaptability in responsive materials and enables reversible changes in biological interactions and sensing capabilities. Therefore, it is crucial to master the control of supramolecular chirality for precise tuning of material properties, which continues to pose significant challenges in controlling the helical direction or even reversing macroscopic chirality. In this regard, altering self-assembly pathways in the aspect of kinetic *vs.* thermodynamic control, which is termed pathway complexity, would be a great option to alter supramolecular chirality by precisely tuning the supramolecular self-

[a]*Centre for Nano and Soft Matter Sciences (CeNS), Shivanapura, Dasanapura Hobli, Bangalore, 562162, India. E-mail: gghosh@cens.res.in*

[b]*Academy of Scientific and Innovation Research (AcSIR), Ghaziabad, 201002, India*

[c]*New Chemistry Unit (NCU), Jawaharlal Nehru Centre for Advanced Scientific Research (JNCASR) Jakkur, Bangalore 560064, India*

[d]*Chemistry and Physics of Materials Unit (CPMU), School of Advanced Materials (SAMat), Jawaharlal Nehru Centre for Advanced Scientific Research (JNCASR) Jakkur, Bangalore 560064, India. E-mail: tmaji@jncasr.ac.in*

† Electronic supplementary information (ESI) available. See DOI: https://doi.org/10.1039/d4sc05016a

‡ These authors contributed equally to this manuscript.

assembly behavior.[23] However, over the past decade, researchers have advanced the field of controlled supramolecular self-assembly in terms of pathway complexity with various π-systems.[11c,23-25] However, controlling the self-assembly process of peptide systems under the guidance of pathway complexity remains a less explored area of research.[25g-j] In this context, short peptide systems equipped with a π-chromophoric unit can serve as optimal molecular components for self-assembly, where nanostructures and functionality can be modulated by varying the external stimulus by engaging various non-covalent interactions. Furthermore, by adjusting various external factors under the guidance of pathway complexity, these non-covalent interactions can be modulated to observe their impact on the chiroptical behavior. Peptides, known for their high biocompatibility, have the potential to mimic natural piezoelectric systems such as collagen and proteins. However, the study of the structure–property relationship of such peptide systems is rare in the literature.[26] In this context, peptide systems provide an environmentally friendly method for producing piezoelectric devices that boast superior flexibility, durability, and responsiveness to mechanical stimuli.[27] We envision that a multi stimuli-responsive small peptide can be self-assembled in a controlled manner to unlock its potential in organic mechano-nanodevices.

Herein, we demonstrate that tetrapeptides appended with naphthalene diimide self-assembled into irregular nanostructures exhibiting a strong circular dichroism (CD) signal, indicative of a specific helical orientation (M-/P-type) associated with kinetically controlled states (KS-I in 100% H_2O and KS-II in 20% DMSO/H_2O). Upon cooling from elevated temperatures to room temperature (RT), a supramolecular chirality switching (P-/M-type) occurred, resulting in the formation of entangled long nanofibers, representing a thermodynamically controlled state (TS) (Scheme 1). Surprisingly, denaturation studies also revealed a supramolecular chirality switching at RT rather than disassembly, even in the presence of over 80% of a good solvent; such an observation has yet to be documented. Furthermore, cosolvent induced studies showed that up to a threshold content of the cosolvent (up to 50%), the system maintained a kinetically controlled state (KS) at RT. In contrast, beyond this threshold, the system directly transitioned into a thermodynamically controlled state (TS) without passing through a kinetic state, which was a rare observation in our view. Finally, we demonstrate the switchable piezoresponsive behavior of self-assembled nanostructures achieved through pathway complexity, which to the best of our knowledge is a scarce observation.[26a]

Results and discussion

Self-assembly studies of NDI-PEP-L

NDI-PEP-L and **NDI-PEP-D** were synthesized by employing the solid phase peptide synthesis method following Fmoc chemistry (the detailed synthesis method is discussed in the ESI†). The self-assembly behavior of both peptides has been investigated by using various spectroscopic and microscopic techniques. The appearance of two sharp absorption bands at 362 nm and 383 nm ($I_{383} > I_{362}$) corresponding to the π–π* transition in UV-vis spectrum of **NDI-PEP-L** in DMSO indicated the monomeric state (Fig. 1a).[28] However, a significant reduction and reversal of the band intensity ($I_{383} < I_{362}$) in H_2O suggested that the self-assembly occurred through strong π–π

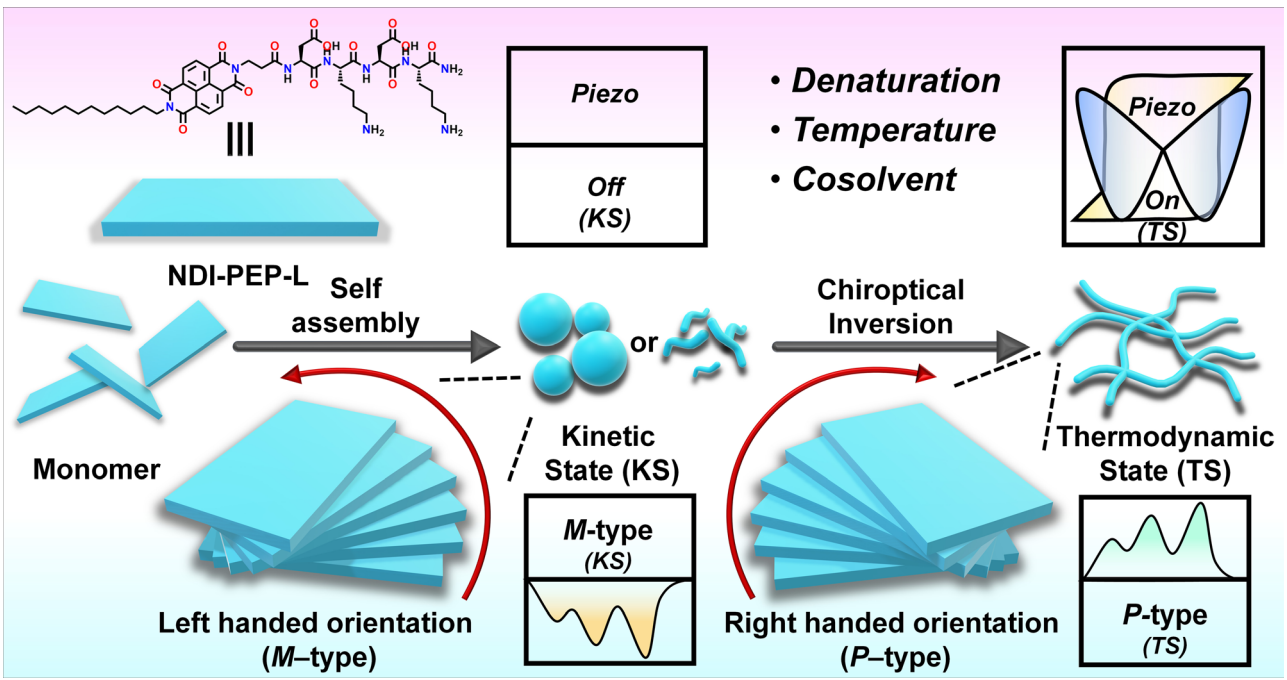

Scheme 1 Schematic representation of chiroptical switching through pathway complexity (kinetic state *vs.* thermodynamic state) in peptide self-assembly influenced by denaturation, temperature and cosolvent and their impact on switchable piezoelectric responses.

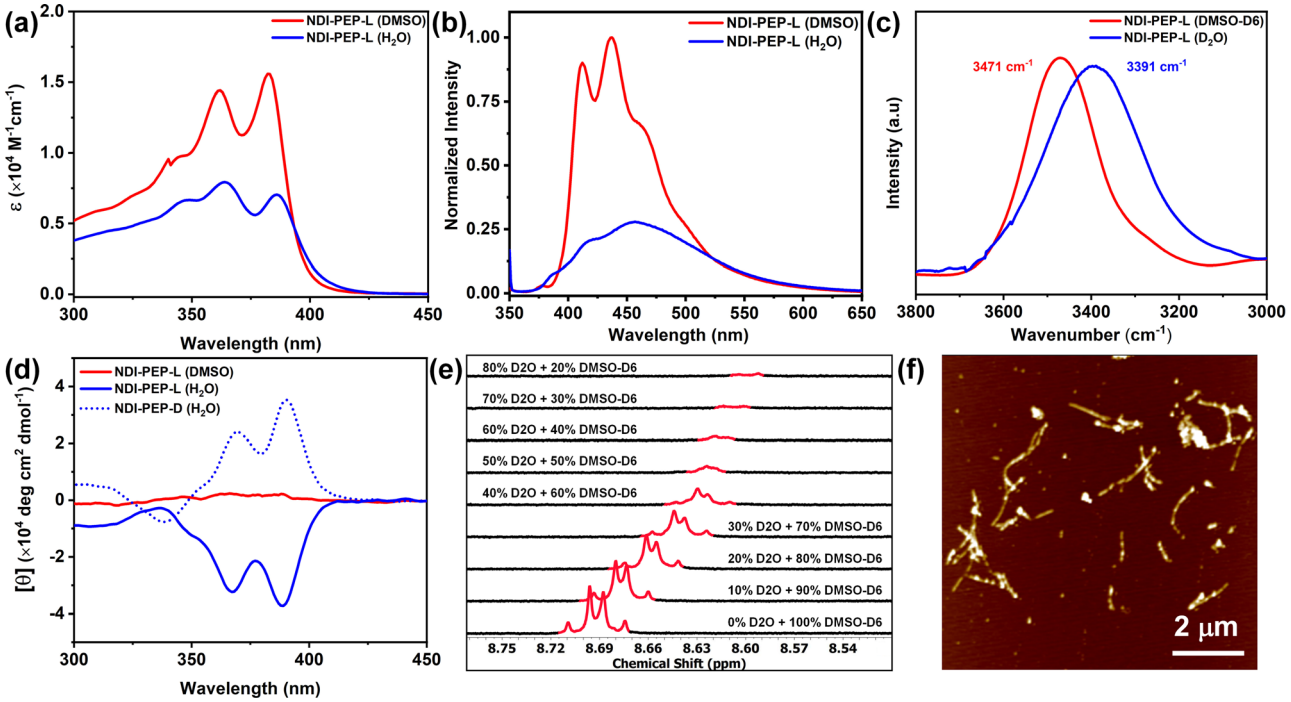

Fig. 1 Solvent-dependent (a) UV-vis spectra; (b) PL spectra; (c) FTIR spectra in the N–H stretching region of **NDI-PEP-L**; (d) CD spectra of **NDI-PEP-L** and **NDI-PEP-D**; (e) ^{1}H-NMR spectra of **NDI-PEP-L** (in the region of aromatic protons) at different % of D_2O; (f) AFM image of **NDI-PEP-L** in H_2O. [C = 0.01 mM for UV-vis, PL, CD, and AFM and C = 1 mM for FTIR and NMR studies].

interactions (Fig. 1a).[28b,29] Photoluminescence (PL) analysis at an excitation wavelength of 360 nm of **NDI-PEP-L** revealed a decrease in emission intensity in H_2O compared to the monomeric state in DMSO, indicating aggregation-caused quenching (ACQ) along with a broad emission band at 456 nm attributed to strong π–π interactions (Fig. 1b). A marked upfield shift and significant broadening of the aromatic protons in ^{1}H-NMR spectra, upon increasing the amount of D_2O (Fig. 1e), further demonstrated the strong π–π interactions.[11c] This phenomenon was further supported by temperature-dependent ^{1}H-NMR studies (DMSO-D_6/D_2O = 1 : 1), where an upfield shift of the naphthalene ring protons was observed upon cooling from 363 K to 293 K (Fig. S9†).[30] H-bonding interactions in the self-assembled state of **NDI-PEP-L**, were indicated by the solvent-dependent FTIR spectra where a prominent peak at 3471 cm^{-1} in DMSO-D_6, suggesting the free N–H stretching of the amide group in the monomeric state (Fig. 1c). However, a significant shift to a lower stretching frequency (at 3391 cm^{-1}) in D_2O,[25h] suggesting strong intermolecular H-bonding interactions. This observation was further corroborated by the notable shift in the amide C=O stretching bands (amide I region), transitioning from the monomeric state (1688 and 1663 cm^{-1}) to the self-assembled state (1669 and 1622 cm^{-1}, respectively) as shown in Fig. S10.† These phenomena demonstrated that the formation of self-assembly in aqueous media occurred through synergistic effects of strong π–π stacking and H-bonding. Importantly, the NDI chromophore and the aliphatic long chain also play a crucial role in the self-assembly process through hydrophobic interactions. Given the tetrapeptide motif in **NDI-PEP-L**, our interest was piqued regarding secondary structure formation during peptide self-assembly. The far UV circular dichroism (CD) studies unveiled a distinct band at 217 nm (Fig. S11†), indicating the formation of a β-sheet rich structure.[11c,d] The FT-IR spectrum of **NDI-PEP-L** revealed two intense peaks at 1622 and 1669 cm^{-1} in the amide-I region, suggesting an intermolecular parallel β-sheet arrangement.[31,11c] Intriguingly, in the UV region, significant negative Cotton effects at 387 and 366 nm corresponding to the NDI chromophore were observed in the CD spectra of **NDI-PEP-L** in H_2O whereas, no CD signal was found in DMSO (Fig. 1d), which is characteristic of the monomeric state. The monosignated CD signal observed in the UV region may be due to induced circular dichroism (ICD) that might have originated from highly asymmetric interactions caused by off-resonance coupling of transition dipoles.[32] Furthermore, we studied the linear dichroism (LD) of **NDI-PEP-L** which revealed an insignificant signal (Fig. S12†), demonstrating the transfer of molecular chirality from the peptide backbone to the supramolecular chirality (macroscopic chirality) during the assembly process.[10c] The negative Cotton effect demonstrated the left-handed (M-type) helical organization of NDI chromophores.[7e,33] To further validate this observation, CD spectrum of the **NDI-PEP-D** isomer, an enantiomer of **NDI-PEP-L**, was recorded under similar condition, showing a positive CD signal (P-type, right-handed helical organization), which was the exact mirror image of the **NDI-PEP-L** CD signal (Fig. 1d). To gain insight into the morphology of **NDI-PEP-L**, we performed atomic force microscopy (AFM), which exhibited the formation of short nanorod like small aggregates (Fig. 1f). Additionally, the dynamic light scattering (DLS) study revealed

a broad particle size distribution, corroborating the formation of anisotropic nanostructures (Fig. S13†).[34]

Temperature-induced chirality switching

To further investigate the mechanistic details of the self-assembly behavior of **NDI-PEP-L**, variable temperature (VT) UV-vis spectroscopic measurement was performed, where no monomeric state was found in H_2O at 363 K (Fig. S14a†), indicating incomplete disassembly even at high temperature. This was further supported by VT-CD where a significant CD signal was noticed at high temperature (Fig. S14b†). These studies suggested the formation of strong aggregates in H_2O, facilitated by strong intermolecular interactions. Short nanorod structures that were observed in H_2O also remained unchanged even upon exposure to heating and subsequent cooling (Fig. S15†). Since reaching the monomeric state was found to be difficult even at high temperature in a poor solvent (H_2O), a 'good and poor solvent' strategy was employed to achieve the monomeric state at elevated temperatures.[35] In this regard, we used 20% DMSO in H_2O where the UV-vis spectral behavior was almost similar to that in 100% H_2O (Fig. S16a†) at RT, indicating no change in the internal order of the chromophores. Upon heating a 0.01 mM solution of **NDI-PEP-L** in 20% DMSO/H_2O at 363 K, a distinct change in both spectral intensity and sharpness was observed, resembling the spectral behavior characteristic of the monomeric state (Fig. S17†). The cooling curve (363 to 298 K, at 1 K min^{-1}) exhibited a non-sigmoidal transition, indicating cooperative supramolecular polymerization (Fig. 2a and b).[11c,28b] The cooling curves at different concentrations (Fig. 2b and S18,† ST1) were analyzed by fitting the data in the nucleation-elongation model,[36] yielding the following parameters: enthalpy (ΔH) = −81.89 kJ mol^{-1}, entropy (ΔS) = −140.1 J mol^{-1} K^{-1}, elongation temperature (T_e) = 349 K (for C = 0.01 mM), Gibbs free energy (ΔG) = −40.23 kJ mol^{-1} and degree of cooperativity (σ) = 2.8 × 10^{-3}. This phenomenon was further supported by CD spectroscopy where a similar Cotton effect was observed in both 100% H_2O and 20% DMSO in H_2O, demonstrating a similar organization of the molecules (Fig. S16b†). Temperature-dependent CD spectra revealed the formation of a CD silent monomeric state upon heating at 363 K (Fig. 2c). It's notable that upon cooling from 363 K to 298 K, the CD signal of **NDI-PEP-L** reversed, suggesting supramolecular chirality switching from the M-type to P-type (from left-handed to right-handed; Fig. 2c) helical assembly. This temperature-assisted stereomutation process was further validated with the stereoisomer, **NDI-PEP-D**. A positive CD signal was observed for a 0.01 mM solution of **NDI-PEP-D** in 20% DMSO/H_2O at RT, which inverted upon heating and subsequent cooling process (Fig. 2d). No such chirality switching (except intensity) was found in the case of 100% H_2O after cooling from 363 K. Slow cooling experiments (from 363 to 298 K at 1 K min^{-1}) in 20% DMSO/H_2O monitored by CD spectroscopy (Fig. 2e) exhibited a non-sigmoidal curve (Fig. 2f), suggesting cooperative supramolecular self-assembly, consistent with the findings from the VT-UV-vis studies. This phenomenon demonstrated the prominent role of temperature in supramolecular chirality inversion.[17]

Interestingly, there was no observable difference in the absorption spectra under similar conditions, suggesting a minimal change in the internal ordering of the overall system during the inversion process (Fig. S17†). The initial aggregate at RT exhibiting a negative CD signal is regarded as the kinetic state (in 100% H_2O as KS-I and 20% DMSO in H_2O as KS-II), while the second aggregate obtained after the thermal annealing process is recognized as the thermodynamic state (TS).[37] An additional investigation was conducted into the stability of the thermodynamically stable state (TS) through thermal annealing, revealing no disassembly even at elevated temperatures. CD

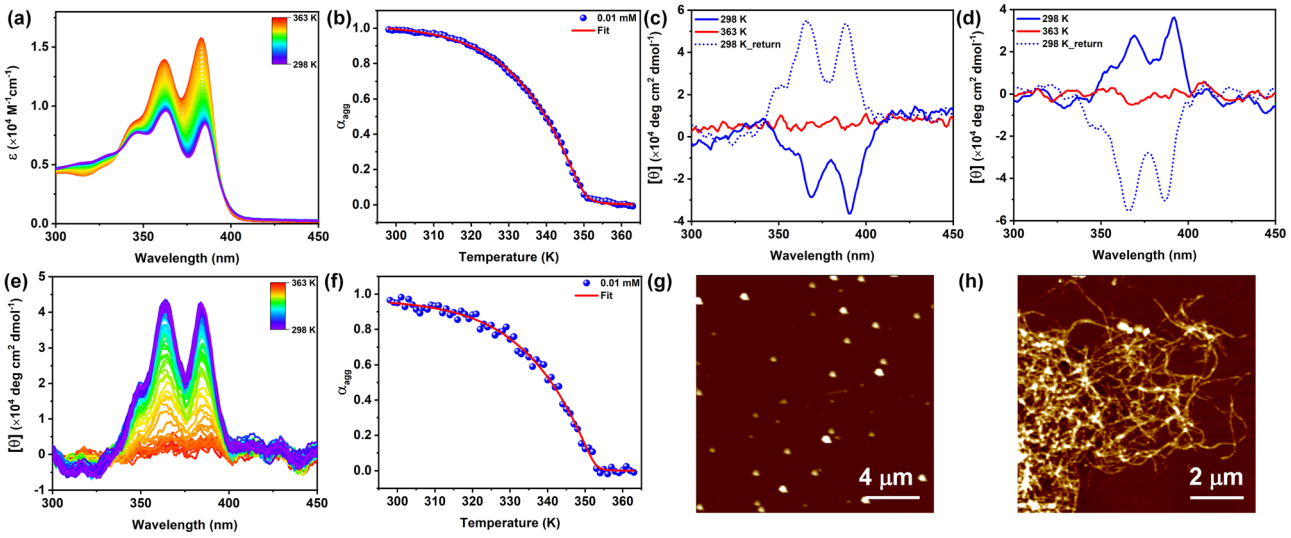

Fig. 2 (a) VT (cooling) UV-vis spectra of **NDI-PEP-L** in H_2O/DMSO (8 : 2) [C = 0.01 mM], (b) cooling curve of **NDI-PEP-L** monitored at 383 nm and fitted to the cooperative model [cooling rate = 1 K min^{-1}], and temperature-dependent (c) CD spectra of **NDI-PEP-L** and (d) **NDI-PEP-D** in H_2O : DMSO (8 : 2) [C = 0.01 mM] indicate disassembly at 363 K and chirality inversion upon cooling back to 298 K. (e) VT (cooling) CD spectra of **NDI-PEP-L** in H_2O/DMSO (8 : 2) [C = 0.01 mM], (f) corresponding cooling curve fitted to the cooperative model [cooling rate = 1 K min^{-1}], and AFM images of **NDI-PEP-L** (g) at RT (KS-II) and (h) after cooling (TS) in H_2O : DMSO (8 : 2).

spectroscopy indicated a slight reduction in the CD signal at high temperatures, which returned to its original position upon cooling to RT (Fig. S19†), suggesting a highly stable aggregated state. In order to gain further insight into the morphological analysis of two different aggregate systems, AFM analysis was carried out under both conditions. KS-II showed the formation of spherical nanoparticles at RT which transformed into highly crosslinked nanofibers (TS) after thermal annealing followed by cooling (Fig. 2g and h). The formation of these nanostructures was confirmed by DLS analysis, which showed a uniform particle size distribution and faster correlation decay kinetics, indicating a smaller, isotropic nanostructure compared to KS I. In the case of TS, a much larger size distribution and slower correlation function decay kinetics supported the formation of higher-order nanostructures (Fig. S20†).[33] Thermal annealing of **NDI-PEP-L** solution in 20% DMSO/H_2O leads to dissociation of the kinetic assembly into monomers and subsequent cooling drives the one directional ordered arrangement of these small peptides into a nanofibrillar structure. The dynamic nature of the non-covalent interactions displayed this kinetic modulation, which regulates the supramolecular chirality through stepwise organization into a thermodynamic aggregate.[10e] The melting curve of the aggregate (KS-II) as determined from UV-vis and CD spectroscopic studies, was found to differ from the cooling curve having higher elongation temperature (Fig. S21 and S22†). The presence of hysteresis with a higher melting point in the heating curve indicated that the system was under kinetic control (Fig. S21b†).[38] Time-dependent CD spectroscopy indicated the absence of chirality inversion over time in both pure H_2O and a 20% DMSO/H_2O mixture, implying the formation of stable kinetic states with substantial energy barriers hindering the transition to the TS at RT (Fig. S23†). The inability to shift from KS-I to TS and the capacity to transition from KS-II to TS upon thermal annealing suggested the significant influence of DMSO (cosolvent) and temperature on the chirality switching process. DMSO has the capacity to disrupt H-bonding, thereby leading to significant conformational changes in such assemblies.[10e] Temperature also plays a crucial role in adjusting the strength of noncovalent interactions like H-bonding and van der Waals forces, which are fundamental in governing the self-assembly behavior of supramolecular systems. By modifying the thermal energy of the system, temperature impacts the kinetic energy of molecules, resulting in alterations in the geometry, orientation, and intensity of noncovalent interactions. Consequently, this temperature-induced adjustment can trigger a reorganization of the building blocks, facilitating the formation of highly stable specific supramolecular structures.[17]

Denaturation-induced chirality switching

The mechanistic understanding of the self-assembly process was clearly elucidated from the cooling curve analysis in the presence of 20% DMSO. As in 100% H_2O, we could not reach the monomeric state even at elevated temperature we were curious to investigate the self-assembly mechanism from KS-I (in 100% H_2O) at RT by the denaturation method using UV-vis and CD spectroscopy. The introduction of a monomeric solution of **NDI-PEP-L** (0.01 mM in DMSO) into the aqueous solution of KS-I resulted in an increase in the absorption intensity of the NDI chromophoric unit. But surprisingly, it failed to reach the monomeric state even after reaching ~83% of the DMSO solvent in the mixture, as evidenced by the spectral characteristics (Fig. 3a). NDI absorption spectra that are highly sensitive towards π–π stacking interaction can be recognized from the intensity ratio of the peaks at 383 and 363 nm. Throughout the denaturation process, a ratio of absorption peaks (I_{383}/I_{363}) lower than 1 was observed (whereas greater than 1 for the monomeric state), indicating the stable aggregated state of **NDI-PEP-L** (Fig. 3a).[28,29] The denaturation study was further investigated with CD spectroscopy under similar conditions. In the initial phase of the denaturation process, a decrease in the intensity of the CD signal was noticed, eventually approaching zero. Intriguingly, upon further increase in the content of cosolvent (DMSO), the CD signal was found to reverse (from a negative CD signal to a positive CD signal), accompanied by an increase in the intensity up to ~78%. The intensity of the CD signal reached a maximum with a saturation point at ~78% (Fig. 3b). To confirm, we further checked the UV-vis spectrum of the final solution obtained after the denaturation study in CD spectroscopy which revealed similar spectral behavior to the UV-vis spectrum obtained before the denaturation study, indicating the presence of the aggregated state (Fig. S24†) even in

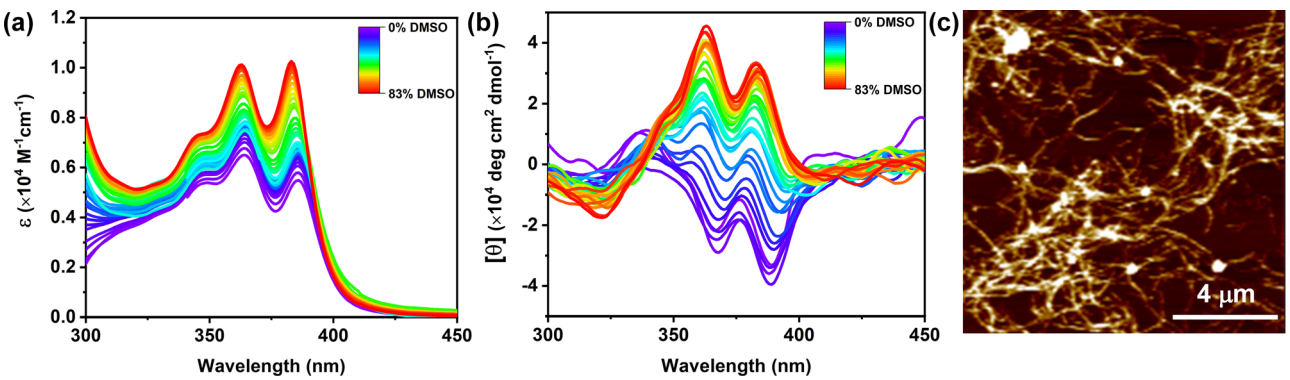

Fig. 3 (a) UV-vis spectra and (b) CD spectra of **NDI-PEP-L** during the denaturation process starting from 100% H_2O [C = 0.01 mM], and (c) AFM analysis after the completion of the denaturation process showing a highly crosslinked nanofibrous structure [C = 0.01 mM].

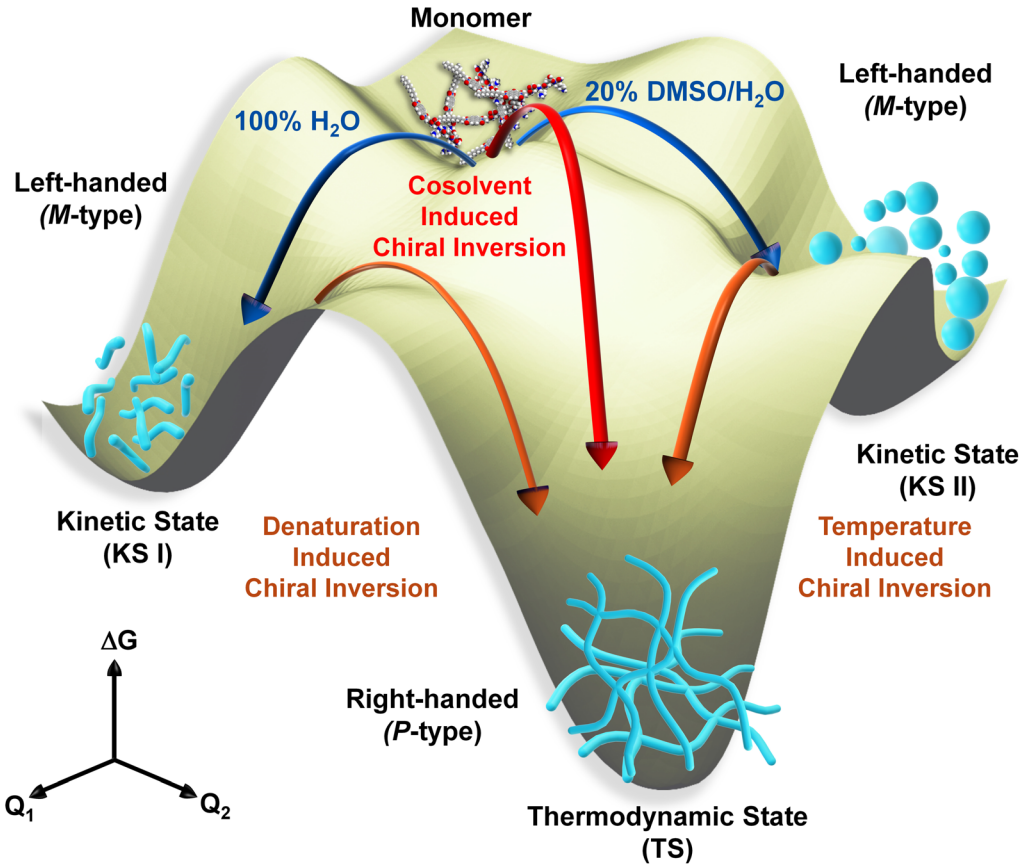

Fig. 4 Qualitative energy surface diagram of the NDI-PEP-L system under different aggregated conditions with different nanostructures in kinetic states (KS-I and KS-II) and the thermodynamic state (TS). Both KS-I and KS-II formed short nanorods and nanoparticles, respectively, with M-type helical orientations which further transformed into TS under different conditions, resulting in the formation of an entangled nanofibrous morphology having P-type helical orientations.

the presence of high cosolvent (DMSO) contents. Thus, the overall denaturation analysis indicated the transformation of the kinetic product (KS-I) to the thermodynamic product (TS), rather than the disassembled state. This chiral switching occurred through a non-chiral aggregated state where the CD signal was almost zero, revealing nanoparticle structures, as confirmed by AFM studies (Fig. S25†). This supramolecular chirality inversion was further validated with the enantiomer (**NDI-PEP-D**), where the positive CD signal inverted into a negative signal, indicating the change in the helical conformation from P- to M-type (Fig. S26†). To the best of our knowledge this kind of denaturation induced supramolecular chirality inversion has yet to be demonstrated. Additionally, to further validate this phenomenon, a fresh 0.01 mM **NDI-PEP-L** solution was prepared in 80% DMSO/H_2O, which showed monomeric spectral characteristics, as evident from UV-vis and CD spectroscopic analysis (no Cotton effect; Fig. S27†). Therefore, it is evident that a slow change in the solvent polarity induces dynamicity in the system, which aided in rearranging the noncovalent interactions and the assembly into a thermodynamically favorable state. However, the direct sample preparation method yielded a monomeric state, as expected, owing to the presence of a high amount of good solvent (cosolvent) in the system. First, the kinetically controlled self-assembly (KS-I) is formed through a rapid aggregation process with an M-type structure, which is stable enough and requires energy to transform into the thermodynamically controlled self-assembled state (TS). In this context, it is feasible to supply the required energy for the transformation, either by heating or through a slow relaxation process, which involves adding a good solvent to the system. The morphological analysis for these two aggregated states was performed through AFM which revealed short nanorod structures in 100% H_2O as the kinetic product (KS-I), which further evolved into cross-linked nanofibrillar architectures (TS) upon completion of the denaturation process (~83% DMSO/H_2O) (Fig. 1d and 3c). These studies suggested the considerably higher stability of the TS even in the presence of a substantial quantity of a good solvent in the system. This nanostructural and conformational transition during denaturation, which involved a change from kinetic to thermodynamic states, further demonstrated the pathway complexity, as observed in previous temperature-studies. These above phenomena associated with intricate pathway complexity were represented in a qualitative energy surface diagram (Fig. 4).

Cosolvent-induced chirality switching

In our investigation into temperature-dependent studies, we observed a significant influence of the cosolvent (DMSO) on

supramolecular chirality switching. Intrigued by this, we delved into understanding how varying amounts of cosolvent affected supramolecular chirality switching (Fig. 4). UV-vis and CD spectra were collected across a range of DMSO percentages, from 0% to 100%. Our findings revealed that **NDI-PEP-L** remained in a stable aggregated state up to a 70% DMSO/H_2O solvent mixture, as indicated by broad absorption maxima and a lower intensity peak observed at 383 nm (Fig. S28†) in UV-vis spectra. CD spectra under similar conditions exhibited negative signals up to 50% DMSO/H_2O, resembling KS-II observed in 20% DMSO/H_2O. Interestingly, a complete inversion of the CD signal was observed after reaching 60% DMSO in H_2O, indicating the direct formation of TS without any KS at RT (Fig. 5a). Further increases in DMSO percentage led to an increase in the CD peak intensity at 70% DMSO/H_2O, followed by a reduction due to higher cosolvent contents. The CD signal approached zero at 80% DMSO/H_2O, signifying complete disassembly of the supramolecular polymer. The inversion of supramolecular chirality occurred within the 50% to 60% DMSO/H_2O solution range, while maintaining the aggregated state throughout the transition process. This transition from the KS to TS occurred through a non-structurally aggregated state, bypassing a monomeric state at RT. **NDI-PEP-L** formed ill-defined nanoparticles in 50% DMSO/H_2O (Fig. S29†), highlighting a transition through a non-chiral aggregated state lacking proper molecular arrangements. This sensitivity to stereomutation underscores the significance of both the presence and threshold concentration of DMSO (here, 50%) required to directly form a TS at RT. This phenomenon was further validated with the **NDI-PEP-D** isomer, exhibiting similar observations with opposite CD signals (Fig. 5b).

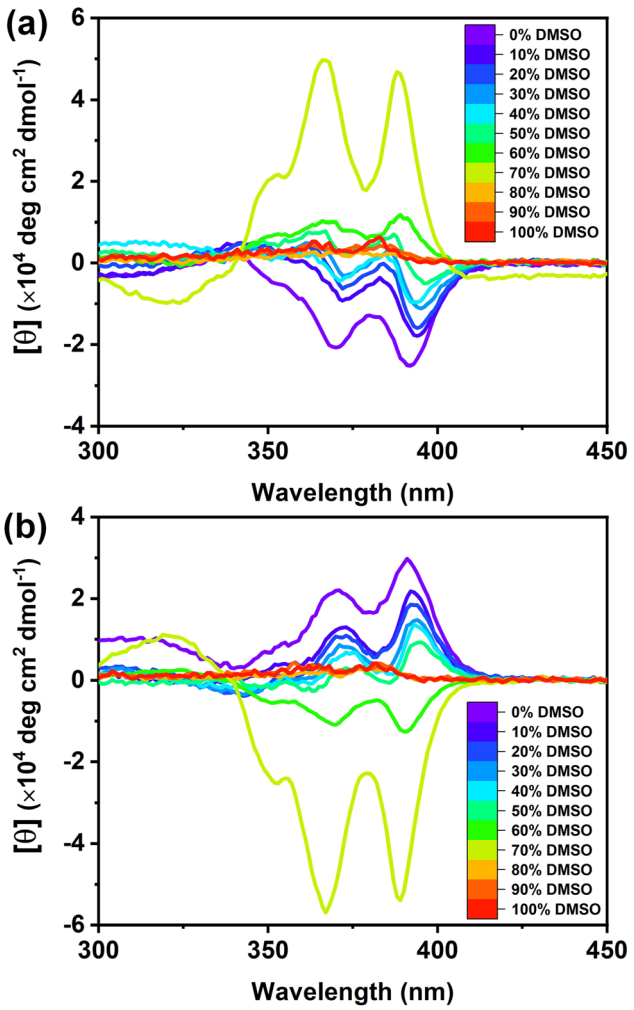

Fig. 5 Cosolvent dependent CD spectra of (a) NDI-PEP-L and (b) NDI-PEP-D [C = 0.01 mM, RT].

Switchable piezo-responsive behavior

Self-assembled peptide systems with a directional H-bonded network are especially intriguing because they generate specific dipole moments throughout the nanoarchitecture. The directional dipolar nature within an anisotropic nanostructure prompted us to investigate the material characteristics of this peptide system under the two distinct aggregated conditions. Self-assembled short peptides are increasingly recognized as adaptable components for creating biocompatible mechanical devices with tailored functionalities. Hence, the possible piezoelectric behavior of the self-assembled **NDI-PEP-L** was examined. Piezo force microscopy (PFM) analysis was carried out for KS-I, KS-II and TS. Samples were prepared on a conducting ITO coated glass substrate and followed by the PFM measurement by monitoring the phase and amplitude alteration upon applying an external electrical bias. The vertical piezoresponse of the peptide nanostructure was evaluated using the piezoelectric coefficient (d_{33}). No piezoresponse was found upon applying the potential for both KS-I and KS-II (Fig. S30,† 6a and b). Interestingly, the TS of **NDI-PEP-L** exhibited a characteristic butterfly loop opening (amplitude curve) (d_{33} = 26.5 pm V^{-1}) (Fig. 6c and S31†). Simultaneously, a distinct 180° phase change was observed, suggesting a shift in the dipolar orientation of the H-bonded amide linkages in response to the applied external potential (Fig. 6d). The piezoresponsive behavior was further confirmed by analyzing the same with the enantiomer. **NDI-PEP-D** also showed similar response towards external bias in its TS (d_{33} = 25.2 pm V^{-1}) (Fig. S32 and S33†). The obtained difference in the piezoresponse of the three different states (KS-I, KS-II and TS) can be attributed to the short range or lower order multidirectional dipolar orientation of the amide linkage in KS-I and KS-II.[26a] In sharp contrast, it's presumed that the TS featured a long-range, unidirectional arrangement of the H-bonded amide connectivity, leading to the emergence of piezo-responsiveness. The thermal annealing process reorganized the peptide system, resulting in the production of more ordered nanostructures with distinct features. The micrometer-long crosslinked nanofibers with well-oriented dipoles, impart an anisotropic quality and generate spontaneous polarization, which can be manipulated under external bias to realize the piezoelectric response. In this context, the M-type helical packing of **NDI-PEP-L** organized the amide functional groups randomly, causing the formation of nanoparticles with nonuniform dipolar orientations. However, in the TS, the P-type helical packing arranged the dipoles in

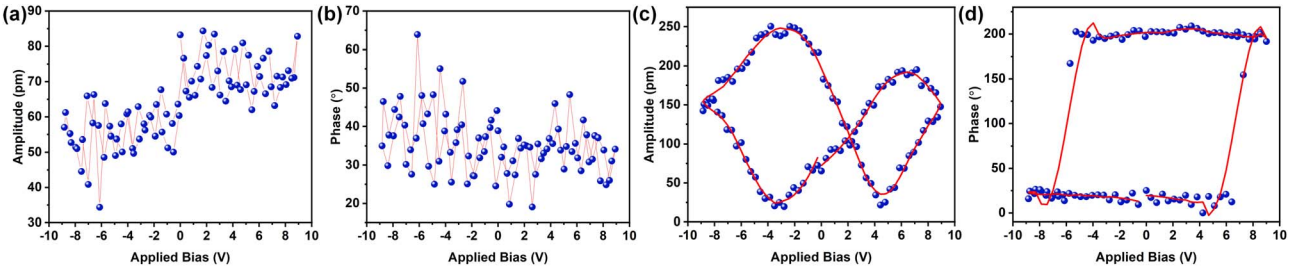

Fig. 6 PFM (a) amplitude voltage butterfly loop (off state) and (b) phase voltage hysteresis loop (off state) obtained for NDI-PEP-L in the kinetically aggregated state (KS II). PFM (c) amplitude voltage butterfly loop (off state) and (d) phase voltage hysteresis loop (off state) obtained for NDI-PEP-L in the thermodynamically aggregated state (TS).

a much more regular pattern, resulting in a consistent dipolar orientation of the amide bonds throughout the fibrillar nanostructure. This phenomenon further illustrates the pivotal influence of specific packing arrangements in constructing self-assembled nanostructures with tunable piezoelectric properties. Although there may not be a direct link between chirality and piezoelectric characteristics, the different nanostructures generated from the KS and TS through pathway complexity are pivotal in driving the observed switchable piezoelectric responses. In our view, the occurrence of switchable piezoresponsive behavior influenced by pathway complexity is a rare and noteworthy phenomenon.[26a]

Conclusion

In summary, our study unveiled the multi-responsive chiroptical switching in peptide self-assembly and switchable piezoelectric responses through pathway complexity. We synthesized a tetrapeptide appended with naphthalene diimide, **NDI-PEP-L** (L-isomer), which self-assembled into kinetically controlled (KS-I) short nanorod structures with an M-type (left-handed) chromophoric organization in H_2O. However, in the presence of a good solvent (cosolvent), specifically 20% DMSO in H_2O, this peptide formed irregular nanoparticles with a similar M-type chromophoric organization, representing another kinetically controlled state (KS-II). Cooling experiments using UV-vis spectroscopy exhibited a cooperative self-assembly mechanism, resulting in the formation of long entangled nanofibers, a thermodynamically stable state (TS). Intriguingly, CD spectroscopy during cooling demonstrated a chiroptical switching from a M-type (left-handed) to a P-type (right-handed) helically organized state, although similar UV-vis spectra were noticed after cooling. Denaturation studies further revealed a surprising observation where a chiroptical switching from a KS (M-type for the L-isomer) to a TS (P-type for the L-isomer) happened rather than a disassembled state even though the system contained over 80% of good solvent (DMSO). This observation represents a novel contribution to the existing literature. Subsequent CD studies, varying the cosolvent (DMSO) content in the aqueous medium, showed that beyond a critical cosolvent content (>50% DMSO), the peptide directly transitioned into a TS (P-type for the L-isomer) at RT, bypassing the kinetic state – also a rare phenomenon in the literature. This unique chiroptical behavior was further supported by similar observations with the enantiomer (D-isomer, **NDI-PEP-D**), which exhibited mirror-image CD signals. This chiroptical switching facilitated the creation of switchable piezoresponsive behavior in peptide-based nanomaterials, highlighting dynamic control over material properties. Essentially, our work pioneered dynamic piezoresponsive control in peptide-based nanomaterials through pathway complexity, opening new avenues for tuning material properties in self-assembled states. Overall, mastery over competing kinetic and thermodynamic pathways offers a route to design adjustable nanostructures with precise dimensions and shapes, pivotal for optimized interactions with biological systems and diverse applications across biomedicine and materials science.

Data availability

The data supporting the findings of this study, including experimental protocols, characterization details, and supplementary figures, have been provided in the ESI.†

Author contributions

G. G. designed the concept of this work. A. R. and T. N. D. performed major experiments and data analysis. G. G. assisted in the data analysis. A. R., T. N. D., T. K. M., and G. G. were involved in the writing and editing of the manuscript. All authors contributed to the preparation of the manuscript.

Conflicts of interest

There are no conflicts to declare.

Acknowledgements

A. R. acknowledges CeNS and DST INSPIRE for the fellowship (DST/INSPIRE/03/2023/002028). T. N. D. acknowledges JNCASR for the fellowship. T. K. M. gratefully acknowledges the Science and Engineering Research Board (SERB), Department of Science and Technology (DST) (Projects SPR/2021/000592) and JNCASR for financial support. The SAMat research facility, Sheikh Saqr Laboratory (SSL) and Sheikh Saqr senior fellowship are also gratefully acknowledged. G. G thanks the Ramanujan Fellowship (file no. RJF/2022/000002), SERB, Government of India and

CeNS (Project no.: CeNSitize-3-GG) for the funding support. A. R. and G. G. also thank the Central Research Facilities of CeNS.

References

1 H. Shigemitsu, T. Fujisaku, W. Tanaka, R. Kubota, S. Minami, K. Urayama and I. Hamachi, An adaptive supramolecular hydrogel comprising self-sorting double nanofibre networks, *Nat. Nanotechnol.*, 2018, **13**, 165–172.

2 (*a*) T. Aida, E. W. Meijer and S. I. Stupp, Functional Supramolecular Polymers, *Science*, 2012, **335**, 813–817; (*b*) C. Roche, H. J. Sun, P. Leowanawat, F. Araoka, B. E. Partridge, M. Peterca, D. A. Wilson, M. E. Prendergast, P. A. Heiney, R. Graf, H. W. Spiess, X. Zeng, G. Ungar and V. Percec, A supramolecular helix that disregards chirality, *Nat. Chem.*, 2016, **8**, 80–89; (*c*) Y. Kim, H. Li, Y. He, X. Chen, X. Ma and M. Lee, Collective helicity switching of a DNA-coat assembly, *Nat. Nanotechnol.*, 2017, **12**, 551–556; (*d*) G. F. Liu, D. Zhang and C. L. Feng, Control of Three- Dimensional Cell Adhesion by the Chirality of Nanofibers in Hydrogels, *Angew. Chem., Int. Ed.*, 2014, **53**, 7789–7793.

3 G. Liu, X. Li, J. Sheng, P. Z. Li, W. K. Ong, S. Z. F. Phua, H. Ågren, L. Zhu and Y. Zhao, Helicity Inversion of Supramolecular Hydrogels Induced by Achiral Substituents, *ACS Nano*, 2017, **11**, 11880–11889.

4 (*a*) M. Liu, L. Zhang and T. Wang, Supramolecular chirality in self-assembled systems, *Chem. Rev.*, 2015, **115**, 7304–7397; (*b*) F. Freire, J. M. Seco, E. Quiñoá and R. Riguera, Chiral Amplification and Helical-Sense Tuning by Mono- and Divalent Metals on Dynamic Helical Polymers, *Angew. Chem., Int. Ed.*, 2011, **50**, 11692–11696; (*c*) M. De Loos, J. Van Esch, R. M. Kellogg and B. L. Feringa, Chiral Recognition in Bis-Urea-Based Aggregates and Organogels through Cooperative Interactions, *Angew. Chem., Int. Ed.*, 2001, **40**, 613–616.

5 (*a*) W. Miao, L. Qin, D. Yang, X. Jin and M. Liu, Multiple-Stimulus- Responsive Supramolecular Gels of Two Components and Dual Chiroptical Switches, *Chem.–A Eur. J.*, 2015, **21**, 1064–1072; (*b*) J. J. D. De Jong, L. N. Lucas and R. M. Kellogg, Reversible Optical Transcription of Supramolecular Chirality into Molecular Chirality, *Science*, 2004, **304**, 278–281.

6 J. Jiang, Y. Meng, L. Zhang and M. Liu, Self- Assembled Single- Walled Metal- Helical Nanotube(M-HN): Creation of Efficient Supramolecular Catalysts for Asymmetric Reaction, *J. Am. Chem. Soc.*, 2016, **138**, 15629–15635.

7 (*a*) Z. Shen, T. Wang, L. Shi, Z. Tang and M. Liu, Strong circularly polarized luminescence from the supramolecular gels of an achiral gelator: tunable intensity and handedness, *Chem. Sci.*, 2015, **6**, 4267–4272; (*b*) H. Wu, Y. Zhou, L. Yin, C. Hang, X. Li, H. Ågren, T. Yi, Q. Zhang and L. Zhu, Helical Self-Assembly-Induced Singlet–Triplet Emissive Switching in a Mechanically Sensitive System, *J. Am. Chem. Soc.*, 2017, **139**, 785–791; (*c*) J. Han, J. You, X. Li, P. Duan and M. Liu, Full-Color Tunable Circularly Polarized Luminescent Nanoassemblies of Achiral AIEgens in Confined Chiral Nanotubes, *Adv. Mater.*, 2017, **29**, 1606503; (*d*) L. Zhu, X. Li, S. Wu, K. T. Nguyen, H. Yan, H. Ågren and Y. Zhao, Chirality Control for in situ Preparation of Gold Nanoparticle Superstructure Directed by Coordinatable Organogelator, *J. Am. Chem. Soc.*, 2013, **135**, 9174–9180; (*e*) C. Liu, D. Yang, Q. Jin, L. Zhang and M. Liu, A Chiroptical Logic Circuit Based on Self-Assembled Soft Materials Containing Amphiphilic Spiropyran, *Adv. Mater.*, 2016, **28**, 1644–1649; (*f*) G. Liu and Y. Zhao, Switching between Phosphorescence and Fluorescence Controlled by Chiral Self-Assembly, *Adv. Sci.*, 2017, **4**, 1700021.

8 G. Song and J. Ren, Recognition and Regulation of unique nucleic acid structures by small molecules, *Chem. Commun.*, 2010, **46**, 7283–7294.

9 C. Soto and S. Pritzkow, Protein misfolding, aggregation, and conformational strains in neurodegenerative diseases, *Nat. Neurosci.*, 2018, **21**, 1332–1340.

10 (*a*) T. Gulik-Krzywicki, C. Fouquey and J. M. Lehn, *Proc. Natl. Acad. Sci. U. S. A.*, 1993, **90**, 163–167; (*b*) M. A. Mateos-Timoneda, M. Crego-Calama and D. N. Reinhoudt, Supramolecular chirality of self-assembled systems in solution, *Chem. Soc. Rev.*, 2004, **33**, 363–372; (*c*) C. C. Lee, C. Grenier, E. W. Meijer and A. P. H. J. Schenning, Preparation and characterization of helical self-assembled nanofibers, *Chem. Soc. Rev.*, 2009, **38**, 671–683; (*d*) H. Miyake and H. Tsukube, Coordination chemistry strategies for dynamic helicates: time-programmable chirality switching with labile and inert metal helicates, *Chem. Soc. Rev.*, 2012, **41**, 6977–6991; (*e*) G. Liu, M. G. Humphrey, C. Zhang and Y. Zhao, Self-assembled stereomutation with supramolecular chirality inversion, *Chem. Soc. Rev.*, 2023, **52**, 4443–4487; (*f*) E. Yashima, N. Ousaka, D. Taura, K. Shimomura, T. Ikai and K. Maeda, Supramolecular Helical Systems: Helical Assemblies of Small Molecules, Foldamers, and Polymers with Chiral Amplification and Their Functions, *Chem. Rev.*, 2016, **116**, 13752–13990.

11 (*a*) B. Yue and L. Zhu, Dynamic Modulation of Supramolecular Chirality Driven by Factors from Internal to External Levels, *Chem.–An Asian J.*, 2019, **14**, 2172–2180; (*b*) S. Huang, Y. Chen, S. Ma and H. Yu, Hierarchical Self-Assembly in Liquid-Crystalline Block Copolymers Enabled by Chirality Transfer, *Angew. Chem., Int. Ed.*, 2018, **57**, 12524–12528; (*c*) G. Ghosh, K. K. Kartha and G. Fernández, Tuning the mechanistic pathways of peptide self-assembly by aromatic interactions, *Chem. Commun.*, 2021, **57**, 1603–1606; (*d*) W. Ji, C. Yuan, P. Chakraborty, S. Gilead, X. Yan and E. Gazit, Stoichiometry-controlled secondary structure transition of amyloid-derived supramolecular dipeptide co-assemblies, *Commun. Chem.*, 2019, **2**, 65.

12 G. Liu, J. Liu, C. Feng and Y. Zhao, Unexpected right-handed helical nanostructures co-assembled from L-phenylalanine derivatives and achiral bipyridines, *Chem. Sci.*, 2017, **8**, 1769–1775.

13 (*a*) X. Zhu, P. Duan, L. Zhang and M. Liu, Regulation of the Chiral Twist and Supramolecular Chirality in Co-Assemblies

of Amphiphilic L-Glutamic Acid with Bipyridines, *Chem.–A Eur. J.*, 2011, **17**, 3429–3437; (*b*) F. Aparicio, B. Nieto-Ortega, F. Najera, F. J. Ramirez, J. T. Lopez Navarrete, J. Casado and L. Sanchez, Inversion of Supramolecular Helicity in Oligo-p-phenylene-Based Supramolecular Polymers: Influence of Molecular Atropisomerism, *Angew. Chem., Int. Ed.*, 2014, **53**, 1373–1377.

14 H. Kashida, K. Murayama, T. Toda and H. Asanuma, Control of the Chirality and Helicity of Oligomers of Serinol Nucleic Acid (SNA) by Sequence Design, *Angew. Chem., Int. Ed.*, 2011, **50**, 1285–1288.

15 R. Lin, H. Zhang, S. Li, L. Chen, W. Zhang, T. Bin Wen, H. Zhang and H. Xia, pH-Switchable Inversion of the Metal-Centered Chirality of Metallabenzenes: Opposite Stereodynamics in Reactions of Ruthenabenzene with L- and D-Cysteine, *Chem.–A Eur. J.*, 2011, **17**, 2420–2427.

16 (*a*) D. Pijper and B. L. Feringa, Molecular Transmission: Controlling the Twist Sense of a Helical Polymer with a Single Light-Driven Molecular Motor, *Angew. Chem., Int. Ed.*, 2007, **46**, 3693–3696; (*b*) D. Pijper, M. G. M. Jongejan, A. Meetsma and B. L. Feringa, Light-Controlled Supramolecular Helicity of a Liquid Crystalline Phase Using a Helical Polymer Functionalized with a Single Chiroptical Molecular Switch, *J. Am. Chem. Soc.*, 2008, **130**, 4541–4552; (*c*) J. Kim, J. Lee, W. Y. Kim, H. Kim, S. Lee, H. C. Lee, Y. S. Lee, M. Seo and S. Y. Kim, Induction and control of supramolecular chirality by light in self-assembled helical nanostructures, *Nat. Commun.*, 2015, **6**, 6959.

17 (*a*) Z. Huang, S. K. Kang, M. Banno, T. Yamaguchi, D. Lee, C. Seok, E. Yashima and M. Lee, *Science*, 2012, **337**, 1521–1526; (*b*) A. Gopal, M. Hifsudheen, S. Furumi, M. Takeuchi and A. Ajayaghosh, Thermally assisted photonic inversion of supramolecular handedness, *Angew. Chem., Int. Ed.*, 2012, **51**, 10505–10509; (*c*) L. Zhang and M. Liu, Supramolecular Chirality and Chiral Inversion of Tetraphenylsulfonato Porphyrin Assemblies on Optically Active Polylysine, *J. Phys. Chem. B*, 2009, **113**, 14015–14020.

18 (*a*) H. Ihara, T. Sakurai, T. Yamada, T. Hashimoto, M. Takafuji, T. Sagawa and H. Hachisako, Chirality Control of Self-Assembling Organogels from a Lipophilic l-Glutamide Derivative with Metal Chlorides, *Langmuir*, 2002, **18**, 7120–7123; (*b*) R. S. Johnson, T. Yamazaki, A. Kovalenko and H. Fenniri, Molecular Basis for Water-Promoted Supramolecular Chirality Inversion in Helical Rosette Nanotubes, *J. Am. Chem. Soc.*, 2007, **129**, 5735–5743; (*c*) T. Ogoshi, T. Akutsu, D. Yamafuji, T. Aoki and T. A. Yamagishi, Solvent- and Achiral-Guest-Triggered Chiral Inversion in a Planar Chiral pseudo[1]Catenane, *Angew. Chem., Int. Ed.*, 2013, **52**, 8111–8115; (*d*) R. Kubota, S. Tashiro and M. Shionoya, Rational synthesis of benzimidazole[3]arenes by CuII-catalyzed post-macrocyclization transformation, *Chem. Sci.*, 2016, **7**, 2217–2221; (*e*) G. Qing, X. Shan, W. Chen, Z. Lv, P. Xiong and T. Sun, Solvent-Driven Chiral-Interaction Reversion for Organogel Formation, *Angew. Chem., Int. Ed.*, 2014, **53**, 2124–2129; (*f*) Y. Huang, J. Wang and Z. Wei, Modulating supramolecular helicity and electrical conductivity of perylene dyes through an achiral alkyl chain, *Chem. Commun.*, 2014, **50**, 8343–8345.

19 (*a*) J. Kumar, T. Nakashima and T. Kawai, Inversion of Supramolecular Chirality in Bichromophoric Perylene Bisimides: Influence of Temperature and Ultrasound, *Langmuir*, 2014, **30**, 6030–6037; (*b*) S. Maity, P. Das and M. Reches, Inversion of Supramolecular Chirality by Sonication-Induced Organogelation, *Sci. Rep.*, 2015, **5**, 16365; (*c*) S. J. Klawa, M. Lee, K. D. Riker, T. Jian, Q. Wang, Y. Gao, M. L. Daly, S. Bhonge, W. S. Childers, T. O. Omosun, A. K. Mehta, D. G. Lynn and R. Freeman, Uncovering supramolecular chirality codes for the design of tunable biomaterials, *Nat. Commun.*, 2024, **15**, 788.

20 (*a*) S. H. Park, S. H. Jung, J. Ahn, J. H. Lee, K. Y. Kwon, J. Jeon, H. Kim, J. Jaworski and J. H. Jung, Reversibly tunable helix inversion in supramolecular gels trigged by Co^{2+}, *Chem. Commun.*, 2014, **50**, 13495–13498; (*b*) Z. Kokan, B. Perić, M. Vazdar, Ž. Marinić, D. Vikić-Topić, E. Meštrović and S. I. Kirin, Metal-induced supramolecular chirality inversion of small self-assembled molecules in solution, *Chem. Commun.*, 2017, **53**, 1945–1948.

21 G. F. Liu, L. Y. Zhu, W. Ji, C. L. Feng and Z. X. Wei, Inversion of the Supramolecular Chirality of Nanofibrous Structures through Co-Assembly with Achiral Molecules, *Angew. Chem., Int. Ed.*, 2016, **55**, 2411–2415.

22 (*a*) L. Gao, X. Dou, C. Xing, F. Gao, Z. Jiang, K. Yang, C. Zhao and C. Feng, Realizing Abundant Chirality Inversion of Supramolecular Nanohelices by Multiply Manipulating the Binding Sites in Molecular Blocks, *Angew. Chem., Int. Ed.*, 2023, **62**, e2023038; (*b*) M. Wehner and F. Würthner, Supramolecular polymerization through kinetic pathway control and living chain growth, *Nat. Rev. Chem*, 2020, **4**, 38–53.

23 P. A. Korevaar, S. J. George, A. J. Markvoort, M. M. J. Smulders, P. A. J. Hilbers, A. P. H. J. Schenning, T. F. A. De Greef and E. W. Meijer, Pathway complexity in supramolecular polymerization, *Nature*, 2012, **481**, 492–496.

24 (*a*) P. A. Korevaar, T. F. A. de Greef and E. W. Meijer, Pathway Complexity in π-Conjugated Materials, *Chem. Mater.*, 2014, **26**, 576–586; (*b*) I. Robayo-Molina, A. F. Molina-Osorio, L. Guinane, S. A. M. Tofail and M. D. Scanlon, Pathway Complexity in Supramolecular Porphyrin Self-Assembly at an Immiscible Liquid-Liquid Interface, *J. Am. Chem. Soc.*, 2021, **143**, 9060–9069; (*c*) L. Herkert, J. Droste, K. K. Kartha, P. A. Korevaar, T. F. A. de Greef, M. R. Hansen and G. Fernández, Pathway Control in Cooperative vs. Anti-Cooperative Supramolecular Polymers, *Angew. Chem., Int. Ed.*, 2019, **58**, 11344–11349; (*d*) J. S. Valera, R. Gómez and L. Sánchez, Kinetic Traps to Activate Stereomutation in Supramolecular Polymers, *Angew. Chem., Int. Ed.*, 2019, **58**, 510–514; (*e*) R. D. Mukhopadhyay and A. Ajayaghosh, Living supramolecular polymerization, *Science*, 2015, **349**, 241–242; (*f*) T. Aizawa, K. Aratsu, S. Datta, T. Mashimo, T. Seki, T. Kajitani, F. Silly and S. Yagai, Hydrogen bond-directed supramolecular polymorphism leading to soft and hard

molecular ordering, *Chem. Commun.*, 2020, **56**, 4280–4283; (*g*) D. Vanderzwaag, T. F. A. De Greef and E. W. Meijer, Programmable Supramolecular Polymerizations, *Angew. Chem., Int. Ed.*, 2015, **54**, 8334–8336; (*h*) G. Ghosh, P. Dey and S. Ghosh, Controlled supramolecular polymerization of π-systems, *Chem. Commun.*, 2020, **56**, 6757–6769; (*i*) A. Das, B. Maity, D. Koley and S. Ghosh, Slothful gelation of a dipolar building block by "top-down" morphology transition from microparticles to nanofibers, *Chem. Commun.*, 2013, **49**, 5757–5759; (*j*) M. J. Mayoral, C. Rest, V. Stepanenko, J. Schellheimer, R. Q. Albuquerque and G. Fernández, Cooperative Supramolecular Polymerization Driven by Metallophilic Pd···Pd Interactions, *J. Am. Chem. Soc.*, 2013, **135**, 2148–2151; (*k*) G. Ghosh and S. Ghosh, Solvent dependent pathway complexity and seeded supramolecular polymerization, *Chem. Commun.*, 2018, **54**, 5720–5723; (*l*) H. Kar, D. W. Gehrig, F. Laquai and S. Ghosh, J-aggregation, its impact on excited state dynamics and unique solvent effects on macroscopic assembly of a core-substituted naphthalenediimide, *Nanoscale*, 2015, **7**, 6729–6736; (*m*) I. Helmers, B. Shen, K. K. Kartha, R. Q. Albuquerque, M. Lee and G. Fernández, Impact of Positional Isomerism on Pathway Complexity in Aqueous Media, *Angew. Chem., Int. Ed.*, 2020, **59**, 5675–5682; (*n*) S. Ogi, V. Stepanenko, K. Sugiyasu, M. Takeuchi and F. Würthner, Mechanism of Self-Assembly Process and Seeded Supramolecular Polymerization of Perylene Bisimide Organogelator, *J. Am. Chem. Soc.*, 2015, **137**, 3300–3307; (*o*) C. Kulkarni, K. K. Bejagam, S. P. Senanayak, K. S. Narayan, S. Balasubramanian and S. J. George, Dipole-Moment-Driven Cooperative Supramolecular Polymerization, *J. Am. Chem. Soc.*, 2015, **137**, 3924–3932; (*p*) A. Jain, S. Dhiman, A. Dhayani, P. K. Vemula and S. J. George, Chemical fuel-driven living and transient supramolecular polymerization, *Nat. Commun.*, 2019, **10**, 450; (*q*) J. Matern, Y. Dorca, L. Sánchez and G. Fernández, Revising Complex Supramolecular Polymerization under Kinetic and Thermodynamic Control, *Angew. Chem., Int. Ed.*, 2019, **58**, 16730–16740; (*r*) A. Sorrenti, J. Leira-Iglesias, A. J. Markvoort, T. F. A. De Greef and T. M. Hermans, Non-equilibrium supramolecular polymerization, *Chem. Soc. Rev.*, 2017, **46**, 5476–5490.

25 (*a*) P. Besenius, Controlling supramolecular polymerization through multicomponent self-assembly, *J. Polym. Sci., Part A: Polym. Chem.*, 2017, **55**, 34–78; (*b*) Z. Huang, B. Qin, L. Chen, J. F. Xu, C. F. J. Faul and X. Zhang, *Macromol. Rapid Commun.*, 2017, **38**, 1700312; (*c*) M. Hartlieb, E. D. H. Mansfield and S. Perrier, A guide to supramolecular polymerizations, *Polym. Chem.*, 2020, **11**, 1083–1110; (*d*) D. Van Der Zwaag, P. A. Pieters, P. A. Korevaar, A. J. Markvoort, A. J. H. Spiering, T. F. A. De Greef and E. W. Meijer, Kinetic Analysis as a Tool to Distinguish Pathway Complexity in Molecular Assembly: An Unexpected Outcome of Structures in Competition, *J. Am. Chem. Soc.*, 2015, **137**, 12677–12688; (*e*) S. Ogi, C. Grzeszkiewicz and F. Würthner, Pathway complexity in the self-assembly of a zinc chlorin model system of natural bacteriochlorophyll J-aggregates, *Chem. Sci.*, 2018, **9**, 2768–2773; (*f*) J. P. Joseph, A. Singh, D. Gupta, C. Miglani and A. Pal, Tandem Interplay of the Host–Guest Interaction and Photoresponsive Supramolecular Polymerization to 1D and 2D Functional Peptide Materials, *ACS Appl. Mater. Interfaces*, 2019, **11**, 28213–28220; (*g*) A. Singh, J. P. Joseph, D. Gupta, C. Miglani, N. A. Mavlankar and A. Pal, Photothermally switchable peptide nanostructures towards modulating catalytic hydrolase activity, *Nanoscale*, 2021, **13**, 13401–13409; (*h*) G. Ghosh, R. Barman, A. Mukherjee, U. Ghosh, S. Ghosh and G. Fernández, Control over Multiple Nano- and Secondary Structures in Peptide Self-Assembly, *Angew. Chem., Int. Ed.*, 2022, **61**, e202113403; (*i*) G. Ghosh, Pathway dependent controlled supramolecular polymerization of peptides, *Giant*, 2023, **14**, 100160; (*j*) P. A. Korevaar, C. J. Newcomb, E. W. Meijer and S. I. Stupp, Pathway Selection in Peptide Amphiphile Assembly, *J. Am. Chem. Soc.*, 2014, **136**, 8540–8543; (*k*) F. Tantakitti, J. Boekhoven, X. Wang, R. V. Kazantsev, T. Yu, J. Li, E. Zhuang, R. Zandi, J. H. Ortony, C. J. Newcomb, L. C. Palmer, G. S. Shekhawat, M. O. De La Cruz, G. C. Schatz and S. I. Stupp, Energy landscapes and functions of supramolecular systems, *Nat. Mater.*, 2016, **15**, 469–476; (*l*) T. N. Das, V. M. T. N. Moram, P. Viswanath, T. K. Maji and G. Ghosh, Controlling Supramolecular Self-Assembly and Nanostructures: A Comparative Study in the Solution Phase and at the Air–Water Interface, *ACS Appl. Nano Mater.*, 2024, **7**, 19311–19319.

26 (*a*) D. Gupta, A. Bhatt, V. Gupta, C. Miglani, J. P. Joseph, J. Ralhan, D. Mandal, M. E. Ali and A. Pal, Photochemically Sequestered Off-Pathway Dormant States of Peptide Amphiphiles for Predictive On-Demand Piezoresponsive Nanostructures, *Chem. Mater.*, 2022, **34**(10), 4456–4470; (*b*) D. Gupta, V. Gupta, D. Nath, C. Miglani, D. Mandal and A. Pal, Stimuli-Responsive Self-Assembly Disassembly in Peptide Amphiphiles to Endow Block-co-Fibers and Tunable Piezoelectric Response, *ACS Appl. Mater. Interfaces*, 2023, **15**, 25110–25121.

27 (*a*) S. Bera, S. Guerin, H. Yuan, J. O'Donnell, N. P. Reynolds, O. Maraba, W. Ji, L. J. W. Shimon, P. A. Cazade, S. A. M. Tofail, D. Thompson, R. Yang and E. Gazit, Molecular engineering of piezoelectricity in collagen-mimicking peptide assemblies, *Nat. Commun.*, 2021, **12**, 2634; (*b*) A. Kholkin, N. Amdursky, I. Bdikin, E. Gazit and G. Rosenman, Strong Piezoelectricity in Bioinspired Peptide Nanotubes, *ACS Nano*, 2010, **4**, 610–614.

28 (*a*) H. Kar, G. Ghosh and S. Ghosh, Solvent Geometry Regulated Cooperative Supramolecular Polymerization, *Chem.–A Eur. J.*, 2017, **23**, 10536–10542; (*b*) G. Ghosh, A. Chakraborty, P. Pal, B. Jana and S. Ghosh, Direct Participation of Solvent Molecules in the Formation of Supramolecular Polymers, *Chem.–A Eur. J.*, 2022, **28**, e202201082; (*c*) A. Chakraborty, G. Ghosh, D. S. Pal, S. Varghese and S. Ghosh, Organobase triggered controlled supramolecular ring opening polymerization and 2D assembly, *Chem. Sci.*, 2019, **10**, 7345–7351.

29 M. R. Molla and S. Ghosh, Structural Variations on Self-Assembly and Macroscopic Properties of 1,4,5,8-Naphthalene-diimide Chromophores, *Chem. Mater.*, 2011, **23**, 95–105.

30 (*a*) D. S. Philips, K. K. Kartha, A. T. Politi, T. Krüger, R. Q. Albuquerque and G. Fernández, Interplay between H-Bonding and Preorganization in the Evolution of Self-Assembled Systems, *Angew. Chem., Int. Ed.*, 2019, **58**, 4732–4736; (*b*) E. E. Greciano, S. Alsina, G. Ghosh, G. Fernández and L. Sánchez, Alkyl Bridge Length to Bias the Kinetics and Stability of Consecutive Supramolecular Polymerizations, *Small Methods*, 2020, **4**, 1900715; (*c*) L. López-Gandul, A. Morón-Blanco, F. García and L. L. Sánchez, Supramolecular Block Copolymers from Tricarboxamides. Biasing Co-assembly by the Incorporation of Pyridine Rings, *Angew. Chemie*, 2023, **135**, e202308749; (*d*) C. Naranjo, S. Adalid, R. Gómez and L. Sánchez, Modulating the Differentiation of Kinetically Controlled Supramolecular Polymerizations through the Alkyl Bridge Length, *Angew. Chemie*, 2023, **135**, e202218572.

31 (*a*) N. Yamada, K. Ariga, M. Naito, K. Matsubara and E. Koyama, Regulation of β-Sheet Structures within Amyloid-Like β-Sheet Assemblage from Tripeptide Derivatives, *J. Am. Chem. Soc.*, 1998, **120**, 12192–12199; (*b*) Y. Zou, Y. Li, W. Hao, X. Hu and G. Ma, Parallel β-Sheet Fibril and Antiparallel β-Sheet Oligomer: New Insights into Amyloid Formation of Hen Egg White Lysozyme under Heat and Acidic Condition from FTIR Spectroscopy, *J. Phys. Chem. B*, 2013, **117**, 4003–4013.

32 (*a*) P. Sharma, A. Venugopal, C. M. Verdi, M. S. Roger, A. Calo` and M. Kumar, Heparin binding induced supramolecular chirality into the self-assembly of perylenediimide bolaamphiphile, *J. Mater. Chem. B*, 2024, **12**, 7292; (*b*) N. S. S. Nizar, M. Sujith, K. Swathi, C. Sissa, A. Painelli and K. G. Thomas, Emergent chiroptical properties in supramolecular and plasmonic assemblies, *Chem. Soc. Rev.*, 2021, **50**, 11208–11226; (*c*) K. G. Thomas, Emergent Chiroptical Properties in Assembled Molecules and Materials: From Native Chirality to Global Chirality, *ECS Meet. Abstr.*, 2024, **MA2024-01**, 940.

33 (*a*) M. Kumar, P. Brocorens, C. Tonnelé, D. Beljonne, M. Surin and S. J. George, A dynamic supramolecular polymer with stimuli-responsive handedness for in situ probing of enzymatic ATP hydrolysis, *Nat. Commun.*, 2014, **5**, 5793; (*b*) G. Ghosh, M. Paul, T. Sakurai, W. Matsuda, S. Seki and S. Ghosh, Supramolecular Chirality Issues in Unorthodox Naphthalene Diimide Gelators, *Chem.–A Eur. J.*, 2018, **24**, 1938–1946; (*c*) H. Shao, T. Nguyen, N. C. Romano, D. A. Modarelli and J. R. Parquette, Self-Assembly of 1-D n-Type Nanostructures Based on Naphthalene Diimide-Appended Dipeptides, *J. Am. Chem. Soc.*, 2009, **131**, 16374–16376.

34 (*a*) M. Joy, S. J. Iyengar, J. Chakraborty and S. Ghosh, Layered double hydroxide using hydrothermal treatment: morphology evolution, intercalation and release kinetics of diclofenac sodium, *Front. Mater. Sci.*, 2017, **11**, 395–409; (*b*) S. Chaturvedi, D. Maheshwari, A. Chawathe and N. Sharma, Current analytical approaches for characterizing nanoparticle sizes in pharmaceutical research, *J. Nanopart. Res.*, 2024, **26**, 19.

35 H. Ma, X. Cheng, G. Zhang, T. Miao, Z. He and W. Zhang, Revealing Pathway Complexity and Helical Inversion in Supramolecular Assemblies Through Solvent-Induced Radical Disparities, *Adv. Sci.*, 2024, **11**, 2308371.

36 (*a*) A. J. Markvoort, H. M. M. Ten Eikelder, P. A. J. Hilbers, T. F. A. De Greef and E. W. Meijer, Theoretical models of nonlinear effects in two-component cooperative supramolecular copolymerizations, *Nat. Commun.*, 2011, **2**, 509; (*b*) H. M. M. Ten Eikelder, A. J. Markvoort, T. F. A. De Greef and P. A. J. Hilbers, An Equilibrium Model for Chiral Amplification in Supramolecular Polymers, *J. Phys. Chem. B*, 2012, **116**, 5291–5301.

37 (*a*) E. E. Greciano, J. Calbo, E. Ortí and L. Sánchez, N-Annulated Perylene Bisimides to Bias the Differentiation of Metastable Supramolecular Assemblies into J- and H-Aggregates, *Angew. Chem., Int. Ed.*, 2020, **59**, 17517–17524; (*b*) D. Görl and F. Würthner, Entropically Driven Self-Assembly of Bolaamphiphilic Perylene Dyes in Water, *Angew. Chem., Int. Ed.*, 2016, **55**, 12094–12098; (*c*) J. Matern, K. K. Kartha, L. Sánchez and G. Fernández, Consequences of hidden kinetic pathways on supramolecular polymerization, *Chem. Sci.*, 2020, **11**, 6780–6788.

38 (*a*) D. D. Prabhu, K. Aratsu, M. Yamauchi, X. Lin, B. Adhikari and S. Yagai, Supramolecular polymerization of hydrogen-bonded rosettes with anthracene chromophores: regioisomeric effect on nanostructures, *Polym. J.*, 2017, **49**, 189–195; (*b*) H. Itabashi, K. Tashiro, S. Koshikawa, S. Datta and S. Yagai, Distinct seed topologies enable comparison of elongation and secondary nucleation pathways in seeded supramolecular polymerization, *Chem. Commun.*, 2023, **59**, 7375–7378.